Adaptive LPQ: An Efficient Descriptor for Blurred Face Recognition

Jun Li, Shasha Li, Jiani Hu and Weihong Deng
School of Information and Communication Engineering, Beijing University of Posts and Telecommunications, Beijing, China

***Abstract*— Local Phase Quantization (LPQ) is a state-of-the-art blur-insensitive texture descriptor. The theoretical and empirical results show that the major energy point of the blurred images depends heavily on the blur type and level, but classical LPQ samples the local patch at predefined frequencies. In this paper, we extend LPQ to Adaptive LPQ (ALPQ) by adaptively setting the sampling frequency for various types of quantized blur kernels, where subspace-based Point Spread Function (PSF) Inference is applied to estimate the blur kernels for the test images. Experimental results on the FERET database (with artificially blurred) and the FRGC database (with real blurred) demonstrate that sampling the local patch at adaptive frequency could largely improve the face recognition performance of LPQ. Moreover, the recognition performance of the proposed ALPQ method is comparable to the state-of-the-art deblurring based methods, such as FADEIN+LPQ.**

I. INTRODUCTION

Automatic face recognition techniques have made great progress with active research in recent years. Most previous methods [1][2][3] achieve highly accurate performance only when recognizing the facial images captured in the ideal imaging conditions. As one of the most common degradations of face images, blur may appear with out-of-focus lens, atmospheric turbulence or relative motion between the cameras and objects. An outstanding challenge it is, blurred face recognition has captured much research attention over the last decade. Existing methods roughly fall into 3 categories:

(1) *Blurring methods* blur the sharp images to match blurred ones. Recently, P.Vageeswaran et.al [9] have proved that all images obtained by blurring an image form a convex set, and proposed a blur-robust algorithm DRBF, which works by blurring the sharp images with the optimal blur kernels and finding the best matches in the LBP feature space. However, problem remains that different individuals tend to appear more similar when blurred[4].

(2) *Deblurring methods*, or image restorations, try to recover the sharp images from blurred ones. Non-blind deblurring methods [10] try to remove blurring assuming knowning the blur kernel (PSF). When it is unknown, deblurring will involve the challenging process of blind deconvolution[13], in which PSF estimation is required. M.Nishiyama et.al [4] revealed that deblurring from a single image is ill-posed and proposed to build multiple PSFs and use the best match as the final predicted PSF. Shortcomings of these methods are the huge time costs during deblurring.

(3) *Blur-invariant Descriptor methods* work on basis of invariants between an sharp image and its blurred ones. Most related works have noticed the invariance of the phase information in the frequency domain[12]. Inspired by Local Binary Pattern (LBP), V.Ojansivu et.al [5] proposed a descriptor Local Phase Quantization, and added some extensions to it[7]. A detailed description of LPQ and its variations could be found in their latest work[8]. LPQ is a local descriptor effective for blurred face recognition, though the experiments of [4] pointed out that the performance of LPQ feature declines dramatically for high blur degrees.

Contributions

Traditional LPQ considers only phase information in the frequency domain, and tries to find a uniform feature based on the phase invariance across blur. However, this is hard to realize since the energy of sampling frequency point varies with changing blur degree. In this paper, we propose to combine the amplitude and phase information together by first inferring the blur PSF and then sampling the best energy point of LPQ feature, so as to extract a much more efficient descriptor, which we call as Adaptive LPQ(ALPQ). Compared with state-of-the-art descriptor LPQ, the new descriptor can: (1) save the trouble of a trade-off between different blur types and blur levels, while (2) greatly improve the average recognition rate across blur. Compared with state-of-the-art deblurring method FADEIN+LPQ, the new descriptor can: (1) shorten the time spent in dealing with a blurred image, and (2) slightly improve the recognition rate.

Outline of the Paper

The rest of the paper is organized as follows: Section(II) describes the basic model and its variations of blur problems, which is the basis for the LPQ and our ALPQ methods. Section(III) first quickly goes through the traditional LPQ feature, and then describes our ALPQ method in details. Section(IV) shows the experimental results on different databases. Section(V) is the conclusion part where some further discussions are presented.

II. BACKGROUND

The blurring process could be modeled as:

$$g(x,y) = (f * h)(x,y) + n(x,y) \tag{1}$$

where $g(x,y)$ is the observed blurred image, $f(x,y)$ the original image, $h(x,y)$ the Point Spread Function (**PSF**). And $n(x,y)$ represents the additive noise resulting from quantization or other camera-induced errors. Here $*$ stands for the convolution operator.

In the frequency domain, term (1) converts to:

$$G(u,v) = (F \cdot H)(u,v) + N(u,v) \tag{2}$$

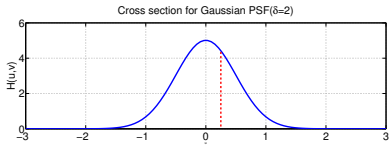

(a) Gaussian PSF

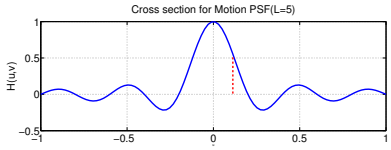

(b) Motion PSF

Fig. 1. Cross sections of different blur PSFs with their sampling points. (a)Gaussian PSF; (b)Motion PSF

We ignore the noise first, for later we will see that the influence of noise would be weakened a lot with sufficient training samples (especially the lower frequency part). Separate the amplitude and phase part, we would get:

$$\begin{aligned} |G(u,v)| &= |F(u,v)||H(u,v)| \\ \angle G(u,v) &= \angle F(u,v) + \angle H(u,v) \end{aligned} \tag{3}$$

If $h(x,y)$ is centrally symmetric,

$$\angle H(u,v) = \begin{cases} 0 & if \quad H(u,v) \geq 0 \\ \pi & if \quad H(u,v) < 0 \end{cases} \tag{4}$$

which means

$$\angle G(u,v) = \angle F(u,v) \quad if \quad H(u,v) \geq 0 \tag{5}$$

In fact, most of the blurred PSFs are centrally symmetric and always satisfy $H(u,v) \geq 0$ in the low frequency parts. Here, we present two common blur PSFs as follows:

(1) *Atmospheric turbulence and out-of-focus blur*, also called as camera focus blur, can be modeled as a gaussian function

$$h(x,y) = e^{-\frac{x^2+y^2}{2\delta^2}} \tag{6}$$

After Fourier Transform, $H(u,v)$ is still gaussian.

$$H(u,v) = \sqrt{2\pi}\delta e^{-\frac{u^2+v^2}{2(\frac{1}{\delta^2})}} \tag{7}$$

Note that the standard deviation becomes $\delta^{'} = \frac{1}{\delta}$ in the frequency domain. $H(u,v)$ is always positive for the whole domain. Fig 1(a) shows the example sampling points in the cross-section of frequency domain for Gaussian PSF.

(2) *Ideal motion blur*, also named as camera motion blur, is caused by relative motion between the object and camera during exposure time. The cross-section of $h(x,y)$ is rectangular. The function along axis x for $h(x,y)$ is:

$$h(x,y) = \begin{cases} \frac{1}{L}, & -\frac{L}{2} \leq x \leq \frac{L}{2}, y = 0 \\ 0, & otherwise \end{cases} \tag{8}$$

L, the "blur length", is proportional to the relative velocity and exposure time. The cross-section of $H(u,v)$ is a sinc function.

$$H(u,v) = \frac{sin(\pi L u)}{\pi L u} = sinc(\pi L u) \tag{9}$$

The value of $H(u,v)$ is always non-negative when $u \leq \frac{1}{L}$. Fig 1(b) shows the example cross-section of Camera Motion PSF and its sampling point.

When the sharp image and its blurred image are compared in the frequency domain, the amplitude part varies with different PSF, while phase part always stay invariant in the low frequency point. The majority of the existing blur related works consider either the phase part or the amplitude part. Our key idea differs from theirs in combining the two parts together to form a much more accurate descriptor.

III. FROM LPQ TO ALPQ

A. Phase Information — Local Phase Quantization

Based on the blur invariance of the Fourier phase part in the low frequency points, V.Ojansivu et.al [5] proposed Local Phase Quantization(**LPQ**) similar to LBP. Here we quickly review the descriptor. Note that in this section we denote $\mathbf{x} = (x,y), \mathbf{u} = (u,v)$ as [5] did.

The local spectra are computed in the $M \times M$ neighborhood N_x of point $\mathbf{x}$, that is, Short-term Fourier Transform(STFT):

$$F(\mathbf{u},\mathbf{x}) = \sum_{\mathbf{y} \in N_x} f(\mathbf{x}-\mathbf{y}) e^{-j2\pi \mathbf{u}^T \mathbf{y}} \tag{10}$$

$\mathbf{u}$ is the observation frequency point, and is chosen to be $\mathbf{u_1} = [a,-a]^T, \mathbf{u_2} = [0,a]^T, \mathbf{u_3} = [a,a]^T, \mathbf{u_4} = [a,-a]^T$, where a is small enough to satisfy $H(\mathbf{u_i}) > 0$. Note that decorrelation is always needed to reduce the correlations between adjacent points. Separate the the real and imaginary parts of $F(\mathbf{u_i},\mathbf{x})$, we could get

$$\begin{aligned} G_x = [&Re\{F(\mathbf{u_1},\mathbf{x}), F(\mathbf{u_2},\mathbf{x}), F(\mathbf{u_3},\mathbf{x}), F(\mathbf{u_4},\mathbf{x})\}, \\ &Im\{F(\mathbf{u_1},\mathbf{x}), F(\mathbf{u_2},\mathbf{x}), F(\mathbf{u_3},\mathbf{x}), F(\mathbf{u_4},\mathbf{x})\}] \end{aligned} \tag{11}$$

$\mathbf{G_x}$ is quantized using a simple scalar quantizer

$$q_j = \begin{cases} 1, & g_j(\mathbf{x}) \geq 0 \\ 0, & otherwise \end{cases} \tag{12}$$

Here $g_j(\mathbf{x})$ is the jth component of $\mathbf{G_x}$. The quantized coefficients are represented as an integer value between 0-255:

$$f_{LPQ}(\mathbf{x}) = \sum_{j=1}^{8} q_j(\mathbf{x}) 2^{j-1} \tag{13}$$

In the rest of the paper, we appoint a as the sampling frequency point. (In fact, it is $\mathbf{u_1}, \mathbf{u_2}, \mathbf{u_3}, \mathbf{u_4}$)

B. Amplitude Information — PSF Inference

The amplitude $|G(u,v)|$ will vary with different blur PSFs if the original face image $F(u,v)$ is aligned to be similar. We adopt the method proposed in [4] to realize PSF inference, which is briefly described as follows.

We first extract feature image $t(\epsilon,\eta)$ from $g(x,y)$ as:

$$t(\epsilon,\eta) = [log(|G(u,v)|)] \downarrow \tag{14}$$

where $[] \downarrow$ stands for down-sampling. Here t is normalized so that $||t||_2 = 1$. Then we run PCA in the training subset, forming correlation matrix $A_i = \frac{1}{M}\Sigma_{k=1}^{M} t_{ik}^{'}(t_{ik}^{'})^T$, where $t_{ik}^{'}$

represents the feature image extracted from image g_{ik} which is blurred with H_i. A subspace $\theta_i = \{b_{ij}\}_{j=1}^{D}$ is obtained with the first D eigenvectors by decreasing eigenvalue. Finally, when comes a new query image with unknown blur, we calculate the closest subspace to determine the PSF H_s by $s = arg\max_i \Sigma_{j=1}^{D}(b_{ij}^T t)^2$.

Fig 2 shows the example extracted features based on the amplitude for different Gaussian blurs.

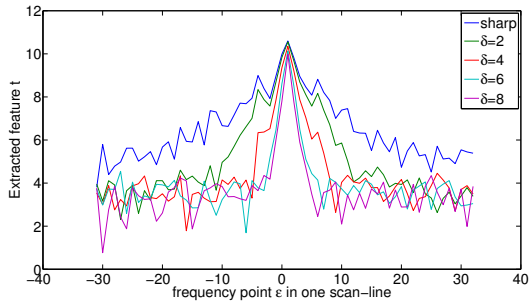

Fig. 2. One scan-line of extracted feature vectors $t(\epsilon, \eta)$ for sharp image $f(x, y)$ and its Gaussian blurred images $g(x, y)$ with standard deviation δ from 2 to 8 in incensement of 2.

C. Combine the two parts together — Adaptive LPQ

Traditional LPQ method sets the sampling frequency point to be fixed for all kinds of blur. We analyzed the phase part of different PSFs and found that there exists a best sample frequency point for a certain blur PSF. Although lower frequency point would be less sensitive to the noise, values that are too small would deteriorate the classification results for sharp features. The key idea of our method is to sample the best frequency points for different blurs adaptively.

The sampling point is set to be $a = \frac{1}{M}$, which means to find the best sampling point is to find the best window size M. Here, M is restricted as $M \in \{3, 5, 7, 9 \ldots\}$ to give a a quantified value. For the gaussian PSF, the standard deviation in the frequency domain is $\delta^{'} = \frac{1}{\delta}$. The energy of the sampling point a is decided by $\frac{a}{\delta^{'}}$, which means $a \sim \delta^{'}$ should be satisfied if we desire the same best sampling energy point. For the camera focus blur, $M \sim \delta$ could be derived from the formulations above. And, for the motion blur, the first zero-cross point is $\frac{1}{L}$. Similarly, an equal energy value can be reached by setting $a \sim \frac{1}{L}$, that is, $M \sim L$.

Considering the uncertain effect of noise $n(x, y)$, we don't try to find exact proportion factor between M and δ or L. We use enough training images to find the mapping relationship between the best window size M and blur PSF parameter, δ or L. We could see from the experiment part that the proportion relationship is approximately satisfied. The chosen STFT windows in the centering point for different blurred images are shown in Fig. 3.

An overview of our method is shown in Fig 4. The best window sizes for different blur types and levels as well as their corresponding subspaces for extracted features are pre-trained in the training procedure with LPQ feature. And in the testing process, the corresponding best window size is chosen with the method of subspace learning-based PSF inference. ALPQ ensures that we always sample the most insensitive phase information in the best frequency point.

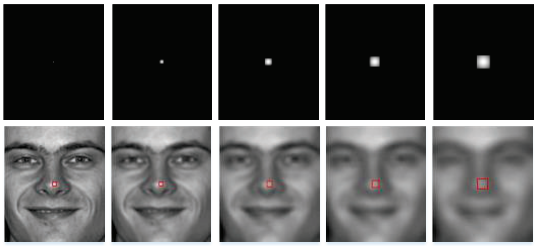

(a) Camera Focus Blur

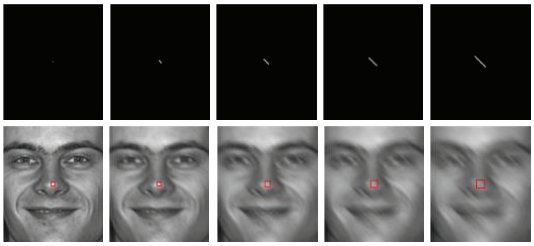

(b) Camera Motion Blur

Fig. 3. Different STFT windows in the centering point of images. For each subgraph, the first row represents the blur kernels (sharp and $\delta = 2$ to 8 in increment of 2 for (a), sharp and $L = 5$ to 20 in increment of 5 for (b)), the second row is the corresponding blurred images, where the red rectangles are the STFT windows in the centering of the images. The blur directions of Motion PSF are fixed to be $\frac{3}{4}\pi$.

IV. EXPERIMENTAL RESULTS

We demonstrate the efficiency of our method (ALPQ) on two publicly available databases, that is, FERET and FRGC 1.0. For both of them, we first crop the face regions, then convert them to gray-scale and resize them to 130*150 pixels. Lastly, the faces are aligned to be with the eyes' positions of $(30, 45), (100, 45)$.

Recently, Nishiyama et.al [4] have proposed to combine PSF Inference + BTV deblur (FADEIN) with LPQ to get a state-of-the-art result for blurred face recognition. We compare our method (ALPQ) with theirs and others' including LPQ (state-of-the-art descriptor) and a Baseline, which is done by directly choosing the raw pixels as features. All of the methods in our experiments use Euclidean Nearest Neighbor as classifiers, for one individual may only have one image in the gallery set. Note that we use Wiener Filter instead of BTV for deblurring. This is because that, firstly, Wiener Filter is about 30 times faster than BTV; secondly, experiments[11] have demonstrated almost the same performances by these two methods; finally, BTV could easily fall into a worse result if the starting point and regularization parameters are set improperly. In fact, FADEIN+LPQ try to solve the decrement with blur levels increasing by deblurring the blurred image to be sharp and setting the window size to be best for sharp images. However, the performance of the method heavily relies on deblurring results and always tends to be slow. ALPQ does not contain deblurring procedure and

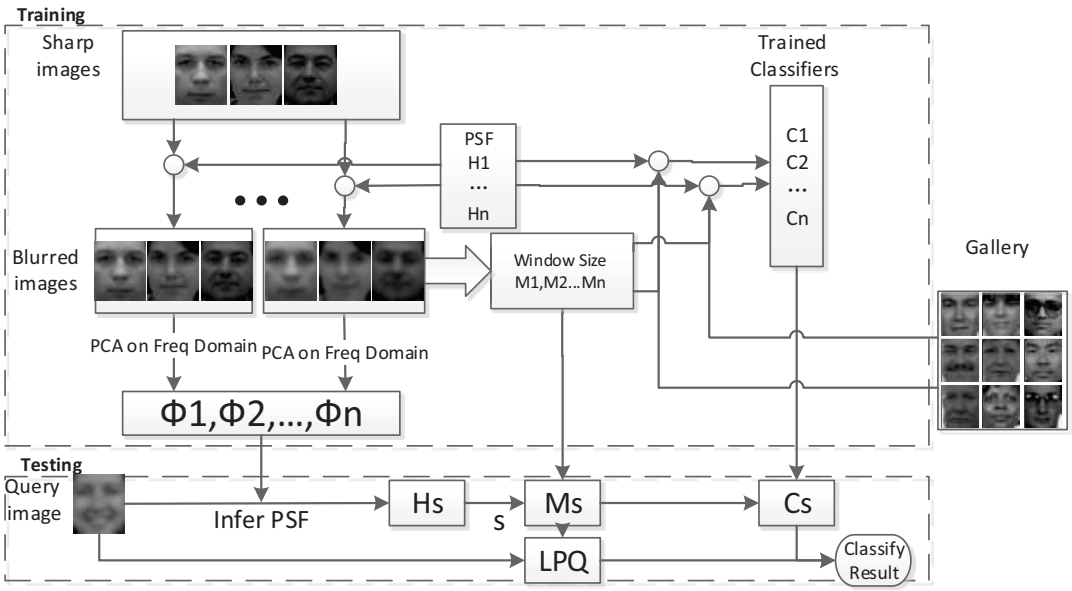

Fig. 4. Overview of Adaptive LPQ.

directly selects the best LPQ feature vector for a certain blur. The following experiments give a fair comparison between them. Experimental results may differ from results reported in [4], owing to some different experiment settings like our faces contain mouths while theirs don't.

A. Artificially blurred database

We first conduct the experiments on synthesized images by artificially blurring sharp images from FERET. We follow the experiment settings of [4] by selecting "bk" subset as the training subset 1 "bj", subset 2, and "ba", subset 3, all contain 200 images and 200 individuals. "fa" subset contains 1196 images and 1196 individuals, "fb" subset 1195 images and 1195 individuals. We first exclude the individuals that have appeared in the training subsets. Then the modified "fa" subset (totaling 996 images) is chosen to be gallery subset, "fb" subset (totaling 995 images) probe subset. All of the images in FERET are sharp.

We introduce two kinds of blur which occur most commonly in the real world, camera focus blur and camera motion blur. The original probe set is artificially blurred to form a new probe set.

1) camera focus blur: The sharp images are blurred with Gaussian PSFs as term (7) presents. White gaussian noise of 30 dB is added to the artificially blurred images. In the training procedure, we use $N = 18$ PSFs, including 17 Gaussian PSFs with standard deviation $\delta = 1$ to 9 in increasement of 0.5, and a "no blur" PSF ($\delta = 0$). It should be mentioned that Gopalan et.al [14] questionably set the filter sizes to be all numerically small ($hsize = 5$) for different standard deviations, while, in fact, the filter size should increase with the standard deviation, or be same but large enough to preserve all of the energy. The gaussian kernel size in our experiments is set to be $2\delta + 1$ first, then around 95% energy would be preserved for all filters. The dimension of each subspace is $D = 20$, and the fixed window size for LPQ is $M = 5$.

LPQ performances with different sampling points

We first blur the training subset 2 with a certain Gaussian PSF with standard deviation $\delta = 0$ to 8 in increasement of 2 respectively. We extract LPQ features with a fixed sampling point on both the blurred training subset 2 and sharp training subset 3, then subset 2 is matched with subset 3 using NN classifier. The LPQ performances on different values of window size M are shown in Fig 5.

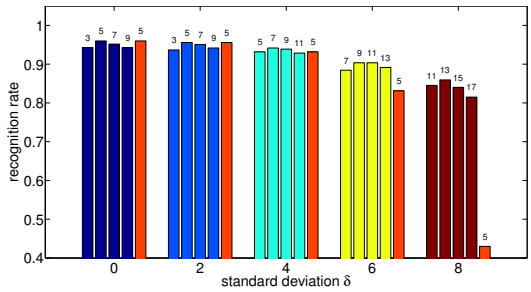

Fig. 5. The recognition rates of LPQ with different sampling points. The figure presents the value near the best sample point for each gaussian PSF. And the last column of each subfigure is our fixed sample point(M=5).

The figure demonstrates that for different PSFs, there exist the best frequency points, which should be the peak for accuracy. Otherwise, either bigger or smaller frequency point would lead to a less desirable recognition performance. However, traditional LPQ set the frequency point to be the same, thus lacking flexibility, and always having to make a trade-off between different PSFs. In ALPQ, we adaptively set M as the best window size M_s. Fig 6 shows the best window size with changing δ learned from training images. Here approximately, $M \sim \delta$, that is, $a \sim \delta^{'}$.

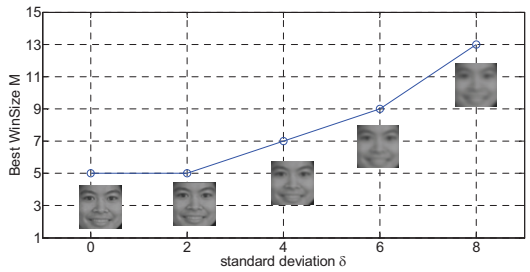

Fig. 6. The best window size with the δ.

TABLE I

PERFORMANCE ON RANDOM CAMERA FOCUS BLUR

Method	Recognition Rate
LPQ	84.8%
FADEIN+LPQ	92.4%
ALPQ	**93.0%**

Performance on different blur PSFs

The experimental settings are the same with the previous one except for that we have no information about the PSF. So PSF Inference is applied and the best frequency point is selected. Comparison between different methods' performances is presented in Fig 7.

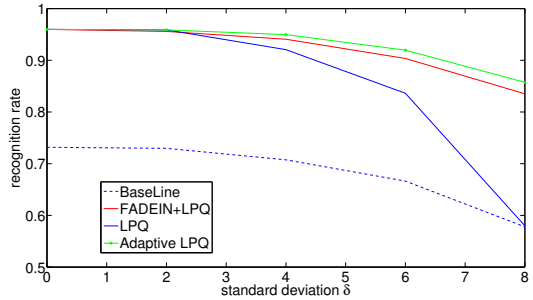

Fig. 7. Comparison between different methods for blurred face recognition with different standard deviation.

Clearly, ALPQ outperforms other methods, especially in the case of Gaussian PSFs with high standard deviation. The reason is that we have made a trade-off trying to match the Gaussian PSFs with lower standard deviation for LPQ feature .

Performance on random blur

We have also tested the face recognition performance when the probe set is blurred with random PSF. This time, every image of the probe set may be blurred by a random gaussian PSF with a standard deviation $\delta \in \{0, 2, 4, 6, 8\}$. The recognition rates are presented in Table I.

2) combine camera motion blur: We then involve camera motion blur. The PSF has been presented in term (9). For the motion blurs, we use PSFs with $L = 2.5$ to 25 in increasement of 2.5 and $\theta = 0, 0.25\pi, 0.5\pi, 0.75\pi$, forming 40 PSFs, then combine a "no blur" PSF to form $N = 41$ PSFs to train the best frequency points of motion blurs.

TABLE II

PERFORMANCE ON COMBINING TWO KINDS OF PSFS.

Method	Average Recognition Rate
LPQ	75.5%
FADEIN+LPQ	78.4 %
ALPQ	**79.6 %**

Similar to gaussian blurs, we could get the relation between the chosen best window size M and motion blur length L, which is presented in Fig 8

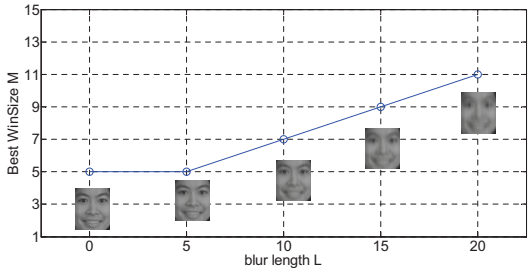

Fig. 8. The best window size with the blur length L.

We put the camera focus blur and camera motion blur together by training $17 + 40 + 1 = 58$ PSFs in the training process. In the testing process, probe images are artificially blurred by Gaussian PSF with $\delta \in \{2, 4, 6, 8\}$ or Motion PSF with $L \in \{5, 10, 15, 20\}, \theta \in \{0, \frac{1}{4}\pi, \frac{1}{2}\pi, \frac{3}{4}\pi\}$. The average recognition rates are shown in Table II.

B. FRGC database with real-world image blur

The last experiment is conducted on images with real blur from FRGC 1.0. We use only the challenging Exp4 that contains uncontrolled still images captured indoors and outdoors for probe set. Note that the gallery set images are captured under carefully controlled condition, which could be definitely considered sharp. Both gallery and probe set contain 943 images from 275 individuals. We have counted by hand that 513 images are blurred in the probe set. Example images are shown in Fig 9.

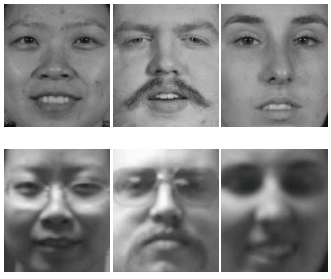

Fig. 9. Example images in FRGC. The first row: gallery images, the second row: probe images with real blur.

The probe images mainly suffer from camera focus blur with the focus on the background. We use $N = 8$ PSFs for training, including 7 Gaussian PSFs with $\delta = 1$ to 4 in

TABLE III

PERFORMANCES UNDER DIFFERENT CONDITIONS (WITH AND WITHOUT ADDED BLURS) ON REAL BLURRED IMAGE FROM FRGC 1.0.4.

Method	original	$\delta_0 = 4$	$\delta_0 = 5$	$\delta_0 = 6$
LPQ	37.8 %	12.4 %	8.2 %	6.3 %
FADEIN+LPQ	38.4 %	14.1 %	8.4 %	6.4 %
ALPQ	**38.9 %**	**15.9 %**	**14.2 %**	**12.2 %**

increasement of 0.5, and a "no blur" PSF($\delta = 0$). Different from previous ones, the filter size is same with the image size ($130 * 150$), which is large enough for the blur PSFs. Three subsets "bk","fa" and "fb" (totaling 2591 images) in FERET are used as training subset to learn 8 subspaces. The dimension of each subspace is $D = 20$.

While a verification is done on FRGC 1.0.4 in [4], this is not proper for us for the dimensions of the feature vectors would change with the inferred PSFs, and a same threshold for distances on different dimension is ill-posed. The performance of face recognition is presented in the second column of Table III. Compared with LPQ, ALPQ and FADEIN+LPQ only help to improve the performance a little, for that the blur levels of FRGC 1.0.4 are small($\delta = 0$ to 4), and that the recognition rate does degrade much with a fixed window size $M = 5$.

We then reconstruct the FRGC database by artificially adding gaussian blurs to the dataset, based on the theory that applying multiple and successive gaussian blurs to an image has the same effect as applying a single larger gaussian blur, whose variance is the sum of the variances that are applied. We separately added gaussian blur with standard deviation of 4,5,6 to the original FRGC probe set, thus forming 3 new probe subsets. For the subset with added standard deviation δ_0, the 8 training PSFs are $\delta = \sqrt{\delta_0^2 + 0^2}, \sqrt{\delta_0^2 + 1^2}, \sqrt{\delta_0^2 + 1.5^2}, \ldots, \sqrt{\delta_0^2 + 4^2}$. Example probe images of the reconstructed subsets are presented in Fig 10. The recognition rate is presented in Table III.

Fig. 10. Example probe images in the reconstructed subsets of FRGC. From left to right: the original probe image with real blur, images with added gaussian blur of standard deviation 4,5,6 respectively.

V. CONCLUSION

We found out the relation between the best sample frequency and blur PSF, and proposed to combine both phase and amplitude parts in the frequency domain to select the best sampling frequency point, which is named as ALPQ. Compared with state-of-the-art method, ALPQ is faster in that no deblurring procedure is involved, and it also turns out to perform better on both artificially blurred database and real blurred database. ALPQ could be viewed as a new descriptor that is capable of greatly enhancing the recognition performance across blur. The limitation of our method is that the gallery images are restricted to be sharp. When the gallery images are not all sharp, however, deblurring methods may be applied to the gallery set. In the future, we consider sampling the frequency point continuously, and also adding other variations like rotation and 3D pose to ALPQ based on the success of LPQ method.

VI. ACKNOWLEDGEMENTS

The authors would like to thank the anonymous reviewers for their thoughtful and constructive remarks that are helpful to improve the quality of this paper. This work was partially sponsored by NSFC (National Natural Science Foundation of China) under Grant No. 61375031, No. 61471048, and No. 61273217. This work was also supported by the Fundamental Research Funds for the Central Universities, Beijing Higher Education Young Elite Teacher Program, and the Program for New Century Excellent Talents in University.

REFERENCES

[1] Weihong Deng, Jiani Hu, Jiwen Lu, Jun Guo, Transform-Invariant PCA: A Unified Approach to Fully Automatic Face Alignment, Representation, and Recognition. *IEEE Transactions on Pattern Analysis and Machine Intelligence (PAMI)*, vol. 36, no. 6, pp. 1275C1284, 2014.

[2] Weihong Deng, Jiani Hu, Jun Guo, Extended SRC: Undersampled Face Recognition via Intra-Class Variant Dictionary, *IEEE Transactions on Pattern Analysis and Machine Intelligence (PAMI)*, vol. 34, no. 9, pp. 1864-1870, 2012.

[3] Weihong Deng, Jiani Hu, Xiuzhuang Zhou, Jun Guo, Equidistant Prototypes Embedding for Single Sample Based Face Recognition with Generic Learning and Incremental Learning, *Pattern Recognition*, vol 47, no. 12, pp. 3738C3749, 2014.

[4] Nishiyama M, Hadid A, Takeshima H, et al. Facial deblur inference using subspace analysis for recognition of blurred faces[J]. *Pattern Analysis and Machine Intelligence*, IEEE Transactions on, 2011, 33(4): 838-845.

[5] Ojansivu, Ville, and Janne Heikkil?. "Blur insensitive texture classification using local phase quantization." *Image and signal processing*. Springer Berlin Heidelberg, 2008. 236-243.

[6] Rahtu, Esa, et al. "Local phase quantization for blur-insensitive image analysis." *Image and Vision Computing* 30.8 (2012): 501-512.

[7] Heikkila, J., and Ville Ojansivu. "Methods for local phase quantization in blur-insensitive image analysis." *Local and Non-Local Approximation in Image Processing*, 2009. LNLA 2009. International Workshop on. IEEE, 2009.

[8] Heikkil?, Janne, Esa Rahtu, and Ville Ojansivu. "Local Phase Quantization for Blur Insensitive Texture Description." *Local Binary Patterns: New Variants and Applications*. Springer Berlin Heidelberg, 2014. 49-84.

[9] Vageeswaran, Priyanka, Kaushik Mitra, and Rama Chellappa. "Blur and illumination robust face recognition via set-theoretic characterization." *Image Processing, IEEE Transactions on* 22.4 (2013): 1362-1372. APA

[10] Fang, Lu, et al. "Separable Kernel for Image Deblurring." *Computer Vision and Pattern Recognition* (CVPR), 2014 IEEE Conference on. IEEE, 2014.

[11] Nishiyama, Masashi, et al. "Facial deblur inference to improve recognition of blurred faces." *Computer Vision and Pattern Recognition*, 2009. CVPR 2009. IEEE Conference on. IEEE, 2009.

[12] Flusser J, Boldys J, Zitov B. Moment forms invariant to rotation and blur in arbitrary number of dimensions[J]. *Pattern Analysis and Machine Intelligence*, IEEE Transactions on, 2003, 25(2): 234-246.

[13] Zheng, Shicheng, Li Xu, and Jiaya Jia. "Forward Motion Deblurring." *Computer Vision (ICCV)*, 2013 IEEE International Conference on. IEEE, 2013.

[14] Gopalan R, Taheri S, Turaga P, et al. A blur-robust descriptor with applications to face recognition[J]. *Pattern Analysis and Machine Intelligence*, IEEE Transactions on, 2012, 34(6): 1220-1226.